

H. Schulz<sup>1</sup>  
M. Baranska<sup>1,2</sup>  
R. Baranski<sup>3,4</sup>

<sup>1</sup> Federal Centre for Breeding  
Research on Cultivated  
Plants (BAZ),  
Institute of Plant Analysis,  
Neuer Weg 22–23, D-06484  
Quedlinburg, Germany

<sup>2</sup> Faculty of Chemistry,  
Jagiellonian University,  
Ingardena 3, 30–060  
Krakow, Poland

<sup>3</sup> Federal Centre for Breeding  
Research on Cultivated  
Plants (BAZ),  
Institute of Horticultural  
Crops,  
Neuer Weg 22–23, D-06484  
Quedlinburg, Germany

---

## Potential of NIR-FT-Raman Spectroscopy in Natural Carotenoid Analysis

<sup>4</sup> Department of Genetics,  
Plant Breeding  
and Seed Science,  
Faculty of Horticulture,  
Krakow Agricultural University,  
Al. 29 Listopada 54, 31–425  
Krakow, Poland

Received 22 September 2004;  
revised 26 October 2004;  
accepted 18 November 2004

Published online 26 January 2005 in Wiley InterScience (www.interscience.wiley.com).  
DOI 10.1002/bip.20215

**Abstract:** This paper demonstrates the special advantages of FT-Raman spectroscopy for *in situ* studies of several carotenoids that occur ubiquitously in the plant kingdom. Spectra obtained from various tissues of a range of plant species indicate that the wavenumber location of C=C stretching vibrations is mainly influenced both by the length as well as by the terminal substituents of the polyene chain of carotenoids and by their interaction with other plant constituents. The obtained results show also the usefulness of Raman spectroscopy in the investigation of *cis*–*trans* isomerization of carotenoids during processing. Additionally, 2-D Raman mappings present a unique possibility to evaluate the individual distribution of carotenoids in the intact plant tissue; in this context different 7-, 8-, and 9-double bond conjugated carotenoids can be analyzed independently in the same sample. Furthermore, the use of Raman spectroscopy for *in situ* detection of unstable substances such as epoxy-carotenoids is discussed. © 2005 Wiley Periodicals, Inc. *Biopolymers* 77: 212–221, 2005

**Keywords:** carotenoids; xanthophylls; epoxy-carotenoids; *in situ*; Raman mapping

## INTRODUCTION

More than 400 carotenoids have been found in higher plants, algae, and bacteria of which  $\alpha$ -,  $\beta$ -carotene, and lutein are uncoun- ted most frequently. The carotenoid color from plants is a precursor for pigmentation in marine animals, egg yolks, and fat globules and serves as a source for vitamin A for mammals.<sup>1</sup> Other biological functions attributed to carotenoids, such as prevention of cancer, cardiovascular disease, and macular degeneration, have been mainly attributed to their antioxidant property.<sup>2–5</sup> The ability of quenching singlet oxygen is related to the conjugated double-bond system and it has been found that maximum protection is given by those having 9 or more double bonds. Thus, in recent years, studies related to human health have focused mainly on 11-conjugated lycopene whereas zeaxanthin and lutein have been investigated in the prevention of age-related macular degeneration.<sup>6–10</sup>

Carotenoids occurring in plants are usually C<sub>40</sub> tetraterpenoids built from eight C<sub>5</sub> isoprenoid units and belong to the class of hydrocarbons (carotenes) or their oxygenated derivatives (xanthophylls). Their distinctive characteristic is a long central chain with a conjugated double-bond system, which is a light-absorbing chromophore responsible for yellow, orange, or red color of these compounds. Although these natural pigments occur in plants as minor components at the ppm level<sup>11</sup> a very sensitive detection can be achieved by Resonance Raman in the visible region, when the wavenumber of the laser excitation coincides with an electronic transition of the individual carotenoid.<sup>12,13</sup> NIR-FT-Raman spectroscopy also gives a strong enhancement of carotenoids due to the known pre-resonance effect; furthermore, the disturbing fluorescence effect of biological material usually observed when laser excitation is performed in the visible wavelength range, is avoided.<sup>11</sup> Strong bands of carotenoids are observed in the Raman spectrum within the 1500–1550 and 1150–1170 cm<sup>-1</sup> ranges due to in-phase C=C ( $\nu_1$ ) and C–C stretching ( $\nu_2$ ) vibrations of the polyene chain. Additionally, in-plane rocking modes of CH<sub>3</sub> groups attached to the polyene chain and coupled with C–C bonds are seen as a peak of medium intensity in the 1000–1020 cm<sup>-1</sup> region. The wavenumber location of these bands, and in particular the  $\nu_1$  band, is strongly dependent on the length of the carotenoid chain,<sup>12,13</sup> but the influence of substituents should also be considered.

Until now, spectrophotometric and liquid chromatographic methods have been extensively applied

for plant pigment analyses.<sup>14–16</sup> Today, high-performance liquid chromatography (HPLC) is mostly used in this context due to its high reproducibility and low detection limit.<sup>17,18</sup> However, application of HPLC requires a long process of sample preparation, including solvent extraction of the pigments, which are usually strongly bonded to other plant constituents (e.g. proteins), and therefore the analysis results may not represent the real (authentic) carotenoid content. Moreover, solvents and also other factors such as high temperature or light may cause changes in the carotenoid conformation, leading to the formation of *cis*-isomers.<sup>1</sup> In nature carotenoids occur primarily as more stable all-*trans*-isomers, thus the presence of *cis*-isomers that are described in the literature as natural products is often overestimated and can be considered to be artefacts. Only a few plant carotenoids are known to be present in the *cis* form, such as phytoene, phytofluene, or bixin.<sup>19,20</sup> Therefore, the in situ analysis of carotenoids that would not affect their conformation is principally of great interest. On the other hand, the described conformational changes of the investigated molecules can be easily monitored by the use of Raman spectroscopy that has already been successfully demonstrated for example in a study of drug polymorphism.<sup>21</sup> In light of the foregoing consideration, NIR-FT-Raman spectroscopy, which is known as a fast and nondestructive method,<sup>22,23</sup> can be a useful and powerful tool for in vivo plant analysis.

In this paper, NIR-FT-Raman spectroscopy is used to analyse carotenoids in situ in intact plant material in which the pigments are present as trace components. It is aimed to obtain spectra that provide reliable information with regard to the structure of the analyzed carotenoids. Moreover, the Raman mapping technique is applied to obtain deeper knowledge of the individual carotenoid distribution in various intact plant tissues.

## MATERIALS AND METHODS

### Sample Material

Naturally occurring carotenoids were analyzed in raw plant tissues of various species listed in Table I. Vegetables (orange carrot roots, red tomato fruits, green French bean pods, broccoli inflorescence, orange pumpkin, corn, and red pepper) as well as fruits (nectarine, apricot, and watermelon) were obtained from the local market. Yellow carrot and basil were cultivated in the experimental garden of the BAZ, whereas flowers of marigold and chamomile, leaves of ivory, begonia, and *Euonymus fortunei* Turcs. were collected from locally growing plants. Saffron stigmas were obtained from Worlee (Hamburg, Germany) and annatto

**Table I** Wavenumber Positions of  $\nu_1$ ,  $\nu_2$ , and  $\nu_3$  Modes of the Predominant Carotenoids Obtained from Measurement of Various Fresh Plant Tissues, Tomato Puree, and Pure Standards by FT-Raman Spectroscopy<sup>a</sup>

| Plant name  | Sample             | $\nu_1$<br>( $\text{cm}^{-1}$ ) | $\nu_2$<br>( $\text{cm}^{-1}$ ) | $\nu_3$<br>( $\text{cm}^{-1}$ ) | Predominant carotenoids              | References |
|---|--------------------|---------------------------------|---------------------------------|---------------------------------|--------------------------------------|------------|
| Saffron <i>Crocus sativus</i> L.  | Dry spice-stigma   | 1536                            | 1165                            | 1020                            | Crocetin (7)                         | 1,25,26    |
| Marigold <i>Calendula officinalis</i> L.  | Petal              | 1536                            | 1157                            | 1007                            | Auroxanthin (7)                      | 45         |
| Marigold <i>Calendula officinalis</i> L.  | Petal/pollen       | 1531–1529                       | 1157                            | 1004                            | Flavoxanthin (8)<br>Luteoxanthin (8) | 45         |
| Chamomille <i>Chamomilla recutita</i> L.  | Pollen             | 1529                            | 1157                            | 1006                            | carotenoid (8)                       |            |
| Marigold <i>Calendula officinalis</i> L.  | Pollen             | 1524                            | 1157                            | 1004                            | Lutein (9)<br>Antheraxanthin (9)     | 45         |
| Nectarine <i>Prunus perica</i> L.<br>var. <i>nucipersica</i><br>(Sucrow) C. Schneid | Fruit              | 1527                            | 1157                            | 1005                            | $\beta$ -Cryptoxanthin (9)           | 1          |
| Carrot <i>Daucus carota</i> L.  | Yellow root        | 1527                            | 1157                            | 1006                            | Lutein (9)                           | 35         |
| Carrot <i>Daucus carota</i> L.  | Leaf               | 1526                            | 1157                            | 1004                            | Lutein (9)<br>$\beta$ -Carotene (9)  | 1          |
| Ivy <i>Hedera helix</i> L.  | Leaf               | 1526                            | 1157                            | 1004                            | Lutein (9)<br>$\beta$ -Carotene (9)  | 1          |
| <i>Euonymus fortunei</i> Turcs.<br>'Canadale Gold'                                  | Leaf               | 1525                            | 1156                            | 1004                            | Lutein (9)<br>$\beta$ -Carotene (9)  | 1          |
| Basil <i>Ocimum basilicum</i> L.  | Leaf               | 1525                            | 1158                            | 1005                            | Lutein (9)<br>$\beta$ -Carotene (9)  | 1          |
| Begonia <i>Begonia x semperflorens-cultorum</i><br>Hort.                            | Leaf               | 1525                            | 1157                            | 1005                            | Lutein (9)<br>$\beta$ -Carotene (9)  | 1          |
| Broccoli <i>Brassica oleracea</i><br>var. <i>italica</i> L.                         | Flower             | 1524                            | 1157                            | 1005                            | Lutein (9)<br>$\beta$ -Carotene (9)  | 1,46       |
| French bean <i>Phaseolus vulgaris</i> L.  | Green pod          | 1524                            | 1157                            | 1005                            | Lutein (9)<br>$\beta$ -Carotene (9)  | 1,47       |
| Corn <i>Zea mays</i> L.   | Seed               | 1522                            | 1157                            | 1005                            | Zeaxanthin (9)                       | 1          |
| Pumpkin <i>Cucurbita pepo</i> L.  | Fruit              | 1524                            | 1157                            | 1009                            | $\beta$ -Carotene (9)                | 1,27       |
| Apricot <i>Prunus armeniaca</i> L.  | Fruit              | 1524                            | 1156                            | 1003                            | $\beta$ -Carotene (9)                | 1          |
| Carrot <i>Daucus carota</i> L.  | Orange root        | 1520                            | 1156                            | 1007                            | $\beta$ -Carotene (9)                | 1,28       |
| Annatto <i>Bixa orellana</i> L.   | Seed               | 1518                            | 1154                            | 1011                            | <i>cis</i> -Bixin (9)                | 1,19,20    |
|   | Seed in chloroform | 1523                            | 1155                            | 1008                            | <i>trans</i> -Bixin (9)              |            |
| Pepper <i>Capsicum annuum</i> L.  | Red fruit          | 1517                            | 1158                            | 1004                            | Capsanthin (9)                       | 1,37–39    |
| Watermelon <i>Citrullus lanatus</i> Thumb.  | Fruit              | 1510                            | 1158                            | 1008                            | Lycopene (11)                        | 1          |
| Tomato <i>Lycopersicon esculentum</i> Mill.   | Fruit              | 1510                            | 1156                            | 1004                            | Lycopene (11)                        | 1,30       |
|   | Puree              | 1510                            | 1156                            | 1006                            | Lycopene (11)                        |            |
| Standard  | Powder             | 1522                            | 1157                            | 1008                            | Lutein (9)                           |            |
| Standard  | Powder             | 1521                            | 1157                            | 1006                            | $\alpha$ -Carotene (9)               |            |
| Standard  | Powder             | 1515                            | 1156                            | 1007                            | $\beta$ -Carotene (9)                |            |

<sup>a</sup>The number of double bonds in conjugated system is shown in parentheses.

seeds were supplied by Martin Bauer & Co. KG GmbH (Vestenbergsgreuth, Germany). Additionally, canned 28% tomato puree (Russo, Italy) was bought in a supermarket.

Pure carotenoid standards ( $\alpha$ -carotene,  $\beta$ -carotene, and lutein) were purchased from Sigma-Aldrich (Taufkirchen, Germany).

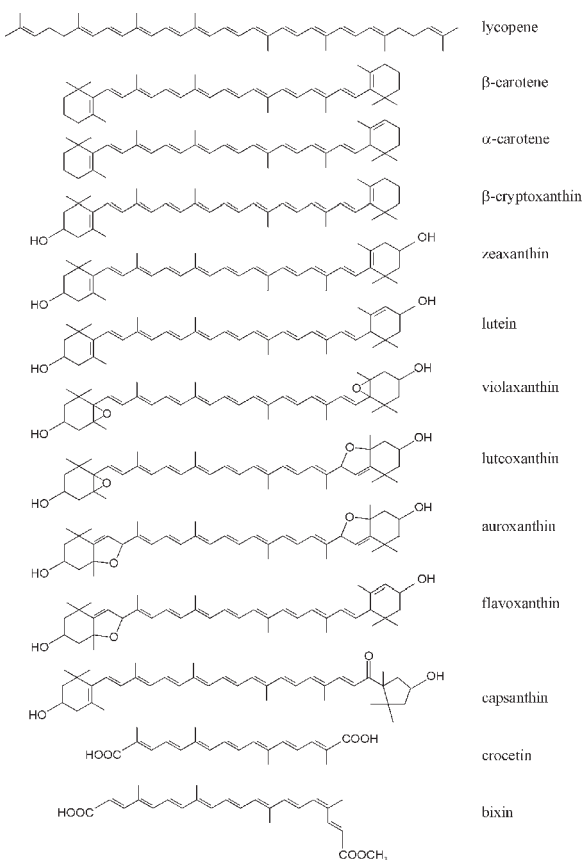


**FIGURE 1** The chemical structure of carotenoids measured and discussed in the paper.

### Raman Measurements

Raman spectra were recorded using a Bruker NIR-FT-Raman spectrometer (model RFS 100) equipped with a Nd:YAG laser, emitting at 1,064 nm, and a germanium detector cooled with liquid nitrogen. The instrument was equipped with an  $xy$  stage, a mirror objective, and a prism slide for redirection of the laser beam. Compared with the standard vertical sampling arrangement, the samples were mounted horizontally.

Spectral measurements were taken from pure carotenoid standard and detached, intact plant organs or their sections. All spectra were measured with a spectral resolution of  $4\text{ cm}^{-1}$  in the range from 100 to  $4000\text{ cm}^{-1}$ . Measurement of fruits and vegetables were performed with 512 scans and an unfocused laser beam of 300 mW, whereas 128 scans and a laser power of 100 mW were used for spectral analysis of leaves, saffron stigmas, and annatto seeds. Carotenoid standards were measured with 128 scans and an unfocused laser beam of 50 mW (for  $\alpha$ - and  $\beta$ -carotene) and of 6 mW (for lutein), respectively.

2-D Raman maps of flat samples were obtained point by point moving the  $xy$  stage;  $x$  and  $y$  directions of the accessory were controlled by the spectrometer software. Traces or 2-D surface areas of the mapped samples were processed

by the Bruker Opus/map software package. Raman mappings of a *E. fortunei* leaf were performed at areas of  $16 \times 12\text{ mm}$  and  $5.5 \times 3.5\text{ mm}$  and marigold flower was mapped at an area of  $26 \times 17\text{ mm}$  with spatial resolutions of 250, 100, and  $250\text{ }\mu\text{m}$ , respectively. These samples were irradiated with a focused laser beam of 100 mW with a diameter of about 0.1 mm, with a spectral resolution of  $4\text{ cm}^{-1}$ ; four scans were collected at each measured point.

## RESULTS AND DISCUSSION

FT-Raman spectroscopy was used for in situ analysis of naturally occurring carotenoids. The chemical structure of predominant carotenoids present in the investigated samples are presented in Figure 1.

### Effect of the Number of Conjugated Double Bonds on the Wavenumber Position of C=C Stretching Vibration

Three naturally occurring carotenoids, crocetin,  $\beta$ -carotene, and lycopene, were chosen as examples to investigate the relationship between  $\nu_1$  wavenumber and the number of conjugated carbon-carbon double bonds present in the polyene chain. For this purpose, FT-Raman measurements were taken from those fresh plant tissues, which are known to contain these pigments as main carotenoids.

Crocetin is a unique 7-conjugated C=C carotenoid substance occurring in stigmas of crocus (*Crocus sativus* L.) flower, which are used as saffron spice. Its golden-yellow coloring matter has long been employed for a food flavoring, whereas, in the Middle Ages, saffron was employed as an artist's colorant.<sup>12,24</sup> In fact, the bright coloring power of saffron comes from the crocins, glycosyl esters of croce-

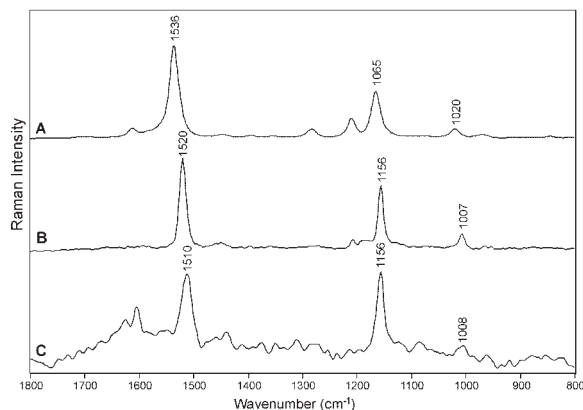


**FIGURE 2** FT-Raman spectra of saffron stigma (A), orange carrot root (B), and red tomato fruit (C).

tin.<sup>25,26</sup> As can be seen in Figure 2A, the  $\nu_1$  band in the FT-Raman spectrum of saffron appears at  $1536\text{ cm}^{-1}$ . This band of crocetin has been previously reported at  $1537\text{ cm}^{-1}$  in the Resonance Raman spectrum<sup>12</sup> and at  $1540\text{ cm}^{-1}$  when excited in a near infrared region.<sup>25</sup> The second intense band in the FT-Raman spectrum of saffron is seen in Figure 2A at  $1165\text{ cm}^{-1}$  and can be attributed to a C–C stretching vibration of the carotenoid skeleton. The in-plane rocking mode of  $\text{CH}_3$  groups attached to the polyene chain is observed as a peak of medium intensity at  $1020\text{ cm}^{-1}$ .

$\beta$ -Carotene, a 9-conjugated C=C carotenoid compound, is the most widespread of all carotenoids in cultivated plants, usually accompanied by  $\alpha$ -carotene at a much lower concentration. Rich sources of  $\beta$ -carotene are orange carrot roots and pumpkin fruits.<sup>27–29</sup> In Figure 2B the FT-Raman spectrum of orange carrot root presents strong bands at  $1520$ ,  $1156$ , and  $1007\text{ cm}^{-1}$ , which can be clearly assigned to  $\nu(\text{C}=\text{C})$ ,  $\nu(\text{C}-\text{C})$ , and  $\tau(\text{CH}_3)$  of  $\beta$ -carotene, respectively.

The principal pigment of red tomato fruits is lycopene, an acyclic 11-conjugated carotene.<sup>29,30</sup> Figure 2C presents the FT-Raman spectrum of tomato; the three most intense bands are seen at  $1510$  ( $\nu_1$ ),  $1156$  ( $\nu_2$ ), and  $1004\text{ cm}^{-1}$  ( $\nu_3$ ). The signal at  $1510\text{ cm}^{-1}$  looks asymmetrical and it can be assumed that the shoulder to be seen at higher wavenumbers (about  $1520\text{ cm}^{-1}$ ) is due to  $\beta$ -carotene, which is also present in tomato but in lower amounts. The assignment of the band registered at  $1510\text{ cm}^{-1}$  is confirmed by Raman measurement of tomato puree rich in lycopene (see Table I). Furthermore, spectra measured in orange tomatoes have shown a higher intensity band near  $1520\text{ cm}^{-1}$  with a shoulder at  $1510\text{ cm}^{-1}$  that corresponds to higher amounts of  $\beta$ -carotene ( $1520\text{ cm}^{-1}$ ) in comparison to lycopene ( $1510\text{ cm}^{-1}$ ), which is reflected also in the color of this vegetable (spectra not presented).

Based on Resonance Raman spectra of retinal, crocetin,  $\beta$ -carotene, lycopene, decapreno- $\beta$ -carotene, and dodecapreno- $\beta$ -carotene it has already been shown that the wavenumber of the  $\nu_1$  band decreases with the extent of the conjugation length of the central polyene chain due to an electron–phonon coupling.<sup>12</sup> Our experiment revealed that this relationship also occurs for carotenoids (i.e., crocetin,  $\beta$ -carotene, and lycopene) measured in situ by FT-Raman spectroscopy. The observed  $\nu_1$  shift toward red is correlated with an increasing number of conjugated double bonds in the carotenoid chain, i.e.,  $1536\text{ cm}^{-1}$  (7)  $\rightarrow$   $1524\text{ cm}^{-1}$  (9)  $\rightarrow$   $1510\text{ cm}^{-1}$  (11). Contrary to that, no correlation is observed for  $\nu_2$  and  $\nu_3$  modes (see

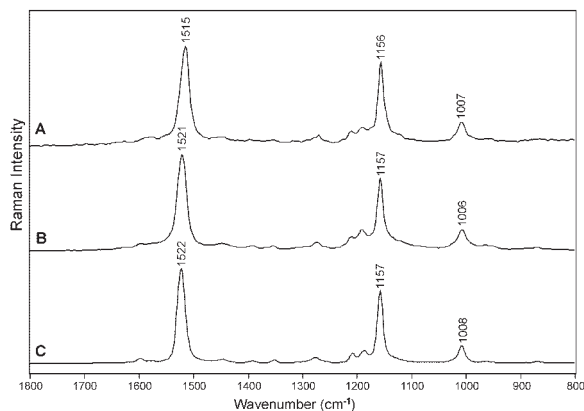


**FIGURE 3** FT-Raman spectra of pure carotenoids standards:  $\beta$ -carotene (A),  $\alpha$ -carotene (B), and lutein (C).

Table I). A similar relationship is observed for other carotenoids as shown in Table I.

### Other Agents Influencing the Wavenumber Location of C=C Stretching Vibration

Cyclization and other modifications during the biosynthetic pathway (hydrogenation, dehydrogenation, isomerization, introduction of hydroxyl groups, rearrangements, etc.) result in a variety of carotenoid structures. Most of them have 9 conjugated double bonds in the central chain. In this study we analyzed three examples of such carotenoids:  $\beta$ -carotene,  $\alpha$ -carotene, and lutein with different side groups. Bicyclic  $\beta$ - and  $\alpha$ -carotenes are formed in two separate branches of the biosynthetic pathway and differ only in the position of the double bond in one  $\beta$ -ionone ring whereas dihydroxylation of the latter results in lutein formation (see Figure 1).

In Figure 3 the FT-Raman spectra of the pure standards ( $\beta$ -carotene,  $\alpha$ -carotene, and lutein) are presented. The wavenumber positions of C=C stretching vibrations are different for the above-mentioned compounds, the lowest is seen for  $\beta$ -carotene at  $1515\text{ cm}^{-1}$ , for  $\alpha$ -carotene at  $1521\text{ cm}^{-1}$ , and at  $1522\text{ cm}^{-1}$  for lutein. All these carotenoids contain the same number of conjugated double bonds, so obviously the regarded wavenumber shift is not correlated with the length of the polyene chain. It can be therefore concluded that the side groups also influence the wavenumber location of  $\nu_1$ .

It was observed that the wavenumber position of the C=C stretching of  $\beta$ -carotene in a pure standard ( $1515\text{ cm}^{-1}$ ) is moved in comparison to that obtained at in situ measurement of carrot roots ( $1520\text{ cm}^{-1}$ ). This phenomenon can be explained by the fact that



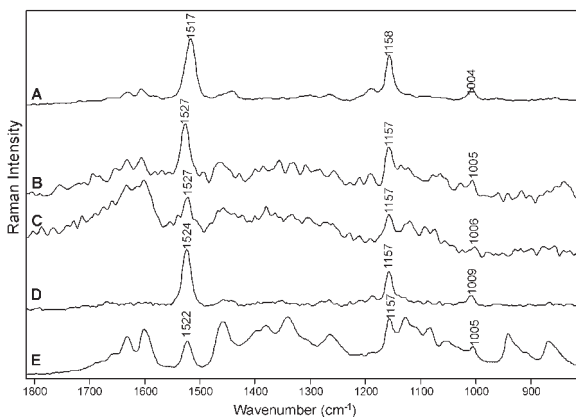


**FIGURE 4** FT-Raman spectra of red pepper fruit (A), nectarine fruit (B), yellow carrot root (C), pumpkin fruit (D), and corn seed (E).

carotenoids in carrot roots are bonded to proteins,<sup>31</sup> but the presence of other carotenoids such as  $\alpha$ -carotene or lutein may also affect the band shift toward higher wavenumbers and therefore cannot be neglected in this context. Generally, chromatographic analyses of carotenoids (TLC, HPLC) in plant tissues include solvent extraction of the pigment. However, this procedure causes the destruction of the natural carotene–protein complexes. Contrary to that, FT-Raman spectroscopy allows the investigation of the carotenoids nondestructively in their natural environment.

In the next step, five carotenoids characterized by 9 conjugated double bonds in the main chain were measured in situ. Figure 4 shows the FT-Raman spectra of red pepper fruit (main carotenoid: capsanthin) (Figure 4A),<sup>32–34</sup> nectarine fruit (main carotenoid:  $\beta$ -cryptoxanthin) (Figure 4B),<sup>1</sup> yellow carrot root (main carotenoid: lutein) (Figure 4C),<sup>35</sup> pumpkin fruit (main carotenoid:  $\beta$ -carotene) (Figure 4D),<sup>27,29</sup> and corn (main carotenoid: zeaxanthin) (Figure 4E).<sup>1,36</sup> For all of these pigments, the characteristic C=C stretching vibration can be found in the wavenumber range between  $1517\text{ cm}^{-1}$  (capsanthin) and  $1527\text{ cm}^{-1}$  (lutein and  $\beta$ -cryptoxanthin). The dispersion of the  $\nu_1$  wavenumbers of 9-conjugated systems is significant, however this wide range is still distinct and is located below  $1536\text{ cm}^{-1}$  (characteristic of the 7-conjugated system of crocetin) and above  $1510\text{ cm}^{-1}$  (characteristic of the 11-conjugated lycopene). These in situ measurements of carotenoids confirm the above-mentioned observation that the side groups of the central polyene chain also influence the position of the  $\nu_1$  wavenumber. The  $\nu_1$  shift can also be attributed to the fact that carotenoids usually bond to other compounds in plants. It is known that green leaves

and vegetables contain unesterified hydroxy carotenoids, mainly lutein, whereas carotenols in fruit are esterified with fatty acids.<sup>1,37–39</sup> In our results lutein can be seen at  $1527\text{ cm}^{-1}$  in yellow carrot root, in green leaves at  $1525\text{--}1526\text{ cm}^{-1}$ , and in green vegetables at  $1524\text{ cm}^{-1}$  (see Table I). A similar situation is observed for  $\beta$ -carotene in orange carrot root ( $1520\text{ cm}^{-1}$ ) and pumpkin or apricot ( $1524\text{ cm}^{-1}$ ).

These examples show that the wavenumber location of C=C stretching is influenced not only by the length of the polyene chain and the molecular structure of the terminal groups of carotenoids but also significantly by their interaction with other plant constituents (proteins, fatty acids, etc.). In this context FT-Raman spectroscopy is a potential tool to perform more detailed investigations of these molecular interactions in situ.

### Cis-Trans Isomerization

Bixin (see Figure 1) is a unique carotenoid compound present in annatto seeds (*Bixa orellana* L.) and it is used in food industry as a natural colorant. Unlike most of the other carotenoids, bixin occurs in nature in the *cis* form, but after extraction in organic solvent it converts to the more stable *trans* form.<sup>20</sup> This experimental observation has already been confirmed by theoretical calculation.<sup>19</sup>

The spectra of bixin obtained directly from seeds as well as related chloroform extracts are presented in Figure 5A and 5B, respectively. As can be seen, the  $\nu_1$  position of bixin occurring in the natural environment is found at  $1518\text{ cm}^{-1}$  whereas in organic solution a band at a higher ( $1523\text{ cm}^{-1}$ ) wavenumber is detected that can be assigned to its two conformational forms, *cis* and *trans*, respec-

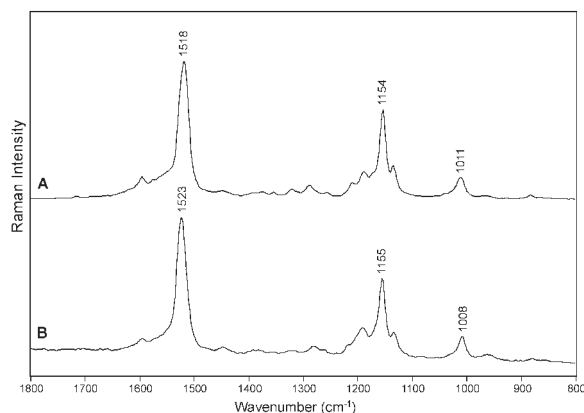


**FIGURE 5** FT-Raman spectra of *cis*-bixin measured directly from annatto seeds (A) and *trans*-bixin in chloroform extract (B).

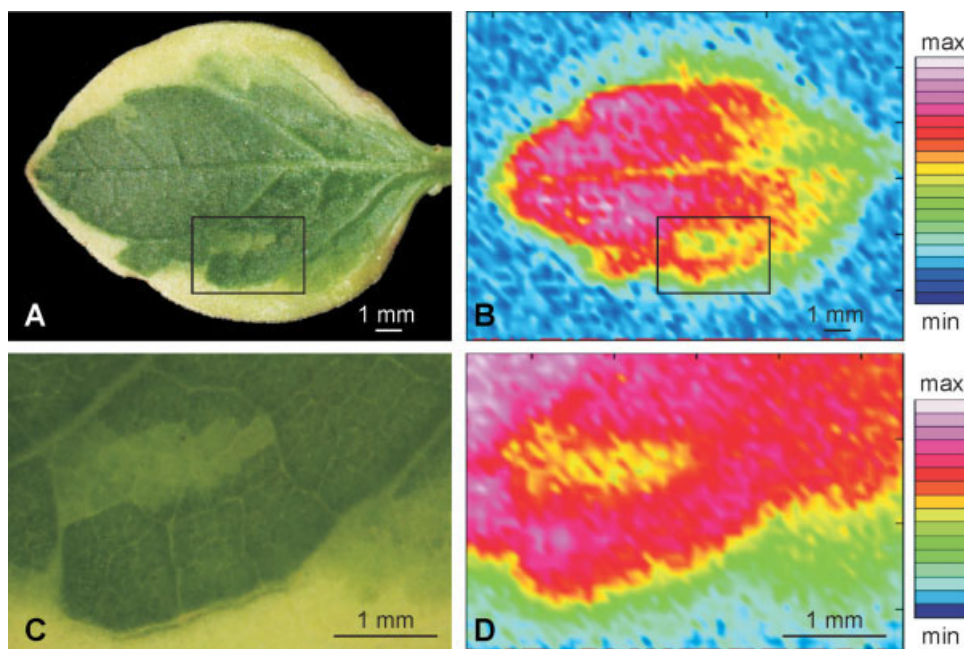


**FIGURE 6** Picture of *Euonymus fortunei* ‘Canadale Gold’ leaf (A), a microscopic image of the defined area (C), and corresponding Raman maps colored according to the intensity of the band at  $1525\text{ cm}^{-1}$ , which represents the total carotenoid content (B and D).

tively. However, some influence of plant constituents bonding to bixin (*cis* isomer) and the chloroform solvent (*trans* isomer) on the  $\nu_1$  position should also be taken into consideration.

FT-Raman spectra of *cis*- and *trans*-crocetin, extracted from *Crocus sativus* L. stigmas and separated by an HPLC method have been previously reported.<sup>26</sup> Stretching vibrations of C=C bonds were observed at  $1535$  and  $1547\text{ cm}^{-1}$  for *trans* and *cis* isomers, respectively. The assignment of these bands is opposite of that discussed above for bixin. Thus, the lower wavenumber of conjugated C=C stretching vibrations is observed for naturally occurring *cis*-bixin in annatto and *trans*-crocetin in crocus.

The difference in the  $\nu_1$  position between *cis* and *trans* isomers in both cases is significant and can be easily detected using FT-Raman spectroscopy. It has already been reported that carotenoids in fruit and vegetables undergo isomerization during processing and/or storage and, as a consequence, a decrease in their color intensity and a reduction of their bioactivity occurs.<sup>1</sup> Heat, light, acids, and adsorption on the metal surfaces promote *trans*–*cis* isomerization, e.g., an increase of *cis*- $\beta$ -carotene can be observed in cooked carrot.<sup>40,41</sup> Therefore, FT-Raman spectroscopy can be efficiently applied for the investigation of conformational changes of carotenoids, e.g., in the field of quality control.

### Raman 2-D Maps of Carotenoid Distribution in Plants

FT-Raman spectroscopy can also be successfully applied to characterize the carotenoid distribution in the plant tissue at cellular level. The use of a horizontal stage with automatically controlled motion provides the opportunity to perform measurements from a specified area of living tissue. As a consequence, a detailed distribution of individual analytes within the measured region in a 2-D map can be visualized.<sup>42–44</sup>

*Euonymus fortunei* Turcs. ‘Canadale Gold’ is a chlorophyll mutant with light green/yellow edge on leaf blades. The presence of yellow carotenoids, mainly lutein, and  $\beta$ -carotene is masked by green chlorophyll, therefore it is not possible to evaluate the carotenoid distribution without analysis. This is why we used Raman mapping to determine the carotenoid distribution in a leaf of *Euonymus*; the relative concentration of carotenoids was determined according to the intensity of the band at  $1525\text{ cm}^{-1}$  (Figure 6). As can be seen, the higher level of carotenoids is observed in dark green leaf regions, which corresponds to a higher amount of chlorophyll in that tissue. A more detailed view was obtained from a second Raman mapping performed over a smaller area of the same leaf but with a higher resolution (Figure 6D). Comparing this map with the related microscopic

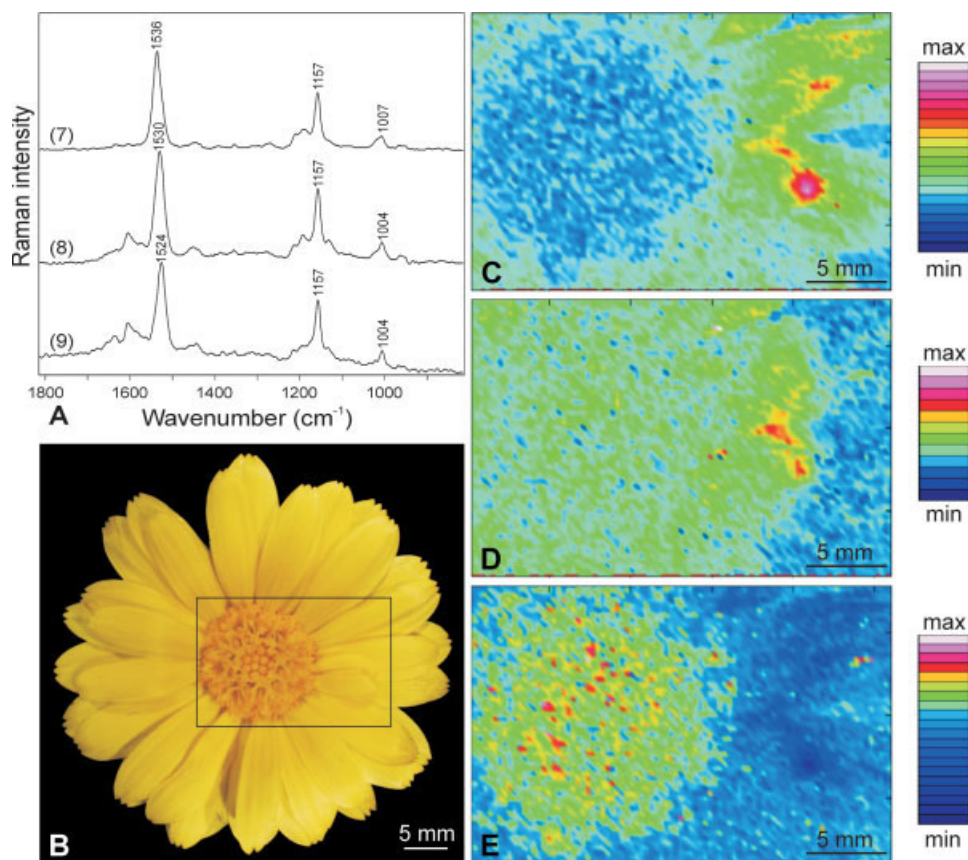


**FIGURE 7** FT-Raman spectra of *Calendula officinalis* L. measured in three different points showing the presence of 7-, 8-, and 9-conjugated carotenoids (A). Picture of *Calendula officinalis* flower (B) and corresponding Raman maps colored according to the band intensity at 1536 (C), 1530 (D), and 1524  $\text{cm}^{-1}$  (E) related to the content of 7-, 8-, and 9-conjugated double bond carotenoids, respectively.

image supplies a rapid overview of the individual carotenoid level corresponding to the anatomical structure of the leaf. This example confirms also the nondestructive feature of NIR-FT-Raman spectroscopy: repeated measurements can be taken from the same sample area several times without perceptible changes with regard to quality or reliability.

On the basis of HPLC investigations it is known that petals and pollen of marigold (*Calendula officinalis* L.) contain mostly flavoxanthin and luteoxanthin (see Figure 1).<sup>45</sup> Luteoxanthin is formed from violaxanthin in the process of epoxidefuranoxide rearrangement, resulting in shortening of the chain to 8 conjugated double bonds. Further epoxidation results in the formation of auroxanthin with a 7-conjugated chain.<sup>1</sup> Auroxanthin is present in marigold petals in high amounts whereas, in the pollen, lutein and antheraxanthin (both pigments are 9-conjugated carotenoids) are additionally detected.<sup>45</sup> The spectra presented in Figure 7A are taken from marigold flower; they show

the different location of the carotenoid  $\nu_1$  bonds. The stretching vibration of C=C bonds of the diepoxy-carotenoid auroxanthin is observed at 1536  $\text{cm}^{-1}$ , exactly at the same wavenumber as for crocetin, the other 7-conjugated system (Figure 7A, upper spectrum). Lutein and anthraxanthin signals are seen at about 1524  $\text{cm}^{-1}$ , which is the characteristic range for 9-conjugated chains (Figure 7A, bottom spectrum). However, the most interesting carotenoids are flavoxanthin and luteoxanthin, as they possess 8 double bonds in the central chain, and, until now, Raman spectra of such systems were not reported. As expected, these carotenoids give strong Raman signals in the range between 1529 and 1531  $\text{cm}^{-1}$  (Figure 7A, middle spectrum). In Figure 7 additionally a photo of marigold flower (Figure 7B) and three Raman maps (Figures 7C, 7D, and 7E) showing the distribution of different carotenoids are presented. The maps were obtained according to the intensities of the characteristic C=C stretching vibrations for 7-,



8-, and 9-conjugated systems, respectively. The presented Raman maps reveal much higher accumulation of auroxanthin in the outer petals and its lack in the inner part of the flower, which is composed mainly of stigmas filled with pollen (Figure 7C). The distribution of lutein and antheraxanthin is opposite, which is in agreement with the performed HPLC measurements (Figure 7E).<sup>45</sup> The derived luteoxanthin with 8-conjugated bonds can be allocated to all flower parts (Figure 7D). However, it is important to stress that the Raman mapping results show the concentration of carotenoids both at the surface and in the surface layer of the flower. The application of NIR laser excitation and lack of confocal arrangement implicate that Raman measurements of the sample may be recorded by penetrating a relatively thick outer layer. This is the reason why, in some parts of *Calendula* flower, where several petals are lying one on the other, a high concentration of carotenoids can be seen (see red spots in Figures 7C and 7D).

The spectrum of *Calendula* pollen with a strong band at about  $1530\text{ cm}^{-1}$  is similar to that measured before<sup>42</sup> in chamomile pollen where the  $\nu_1$  mode was observed at  $1529\text{ cm}^{-1}$  (see Table I). Therefore it is most likely that both flowers contain 8-conjugated epoxy-carotenoids in their pollen.

In conclusion, the presented Raman maps performed in situ allow the precise localization of various carotenoids in different parts of the plant tissue and principally a semiquantitative characterization of these pigments can be achieved. Raman spectroscopy also confirms the presence of 8- and 7-conjugated carotenoids in the *Calendula* flower, most likely flavoxanthin, luteoxanthin, and auroxanthin. These data also show the possibility that FT-Raman spectroscopy can be applied for the measurement of epoxy-carotenoids in situ, which can be very helpful as these compounds have the tendency to easily undergo a degradation and therefore are often underestimated in conventional food or plant analysis. Their occurrence in nature is also often questioned as some of them can be formed as artefacts during sample extraction or analysis.<sup>1</sup>

## CONCLUSION

It has been found that FT-Raman spectroscopy can be successfully applied for the identification of carotenoids directly in the plant tissue without any preliminary sample preparation. Compared with the very intense carotenoid signals the spectral impact of the surrounding biological matrix is weak and therefore does not contribute significantly to the obtained re-

sults. The analysis of natural products (e.g., fruits, vegetables, flowers) can be performed fast, reliably, and nondestructively. The wavenumber locations of different carotenoid C=C stretching vibration are strongly correlated with the individual number of conjugated double bonds but are also influenced by the terminal groups of the polyene chain as well as their interaction with other plant constituents. Additionally, Raman spectroscopy provides structural information about conformational changes of *cis-trans* isomers that may occur during sample preparation or food processing. Furthermore, it is possible to measure unstable epoxy-carotenoids in situ which may easily undergo degradation processes and are therefore underestimated when conventional analytical methods such as HPLC are applied. FT-Raman mapping allows the localization of carotenoids throughout the surface layer of the plant tissue as well as the performance of semiquantitative measurements. Generally, FT-Raman spectroscopy is a powerful and supplementary tool that, in addition to other analytical techniques, can provide very informative data of carotenoids in plant material as well as in related food products.

The financial support of the "Deutsche Forschungsgemeinschaft (DFG)" in Bonn, Germany (grant number: Schu 577/7-1) is gratefully acknowledged.

## REFERENCES

- Rodriguez-Amaya, D. B. *A Guide to Carotenoid Analysis in Food*; ILSI Press: Washington, DC, 2001.
- Maoka, T.; Mochida, K.; Kozuka, M.; Ito, Y.; Fujiwara, Y.; Hashimoto, K.; Enjo, F.; Ogata, M.; Nobukuni, Y.; Tokuda, H.; Nishino, H. *Cancer Lett* 2001, 172, 103–109.
- Kris-Etherton, P. M.; Hecker, K. D.; Bonanome, A.; Coval, S. M.; Binkoski, A. E.; Hilpert, K. F.; Griel, A. E. *Etherton, T. D. Am J Med* 2002, 30, 71–88.
- Garland, M.; Fawzi, W. W. *Nutr Res* 1999, 19, 1259–1276.
- Burri, B. J. *Nutr Res* 1997, 17, 547–580.
- McLaren, D. S. *Newsletters* 2000, 2, 17–18.
- Landrum, J. T.; Bone, R. A. *Arch Biochem Biophys* 2001, 385, 28–40.
- Schalch, W. *Newsletter* 2000, 2, 3–10.
- Rao, A. V.; Agarwal, S. *Nutr Res* 1999, 19, 305–323.
- Bramley, P. M. *Phytochemistry* 2000, 54, 233–236.
- Ozaki, Y.; Cho, R.; Ikegawa, K.; Muraishi, S.; Kawachi, K. *Appl Spectrosc* 1992, 46, 1503–1507.
- Withnall, R.; Chowdhry, B. Z.; Silver, J.; Edwards, H. G. M.; de Oliveira L. F. C. *Spectrochim Acta A* 2003, 59, 2207–2212.

13. Veronelli, M.; Zerbi, G.; Stradi, R. *J Raman Spectrosc* 1995, 26, 683–692.
14. Schoefs, B. *Trends Food Sci Tech* 2002, 13, 361–371.
15. Sander, L. C.; Sharpless, K. E.; Pursch, M. *J Chromatogr A* 2000, 880, 189–202.
16. Cserháti, T.; Forgacs, E. *J Chromatogr A* 2001, 936, 119–137.
17. Breithaupt, D. E. *Food Chem* 2004, 86, 449–456.
18. Belie, N. D.; Pedersen, D. K.; Martens, M.; Bro, R.; Munck, L.; Baerdemaeker, J. *Biosystems Eng* 2003, 85, 213–225.
19. De Oliveira, L. F. C.; Dantas, S. O.; Velozo, E. S.; Santos, P. S.; Ribeiro, M. C. C. *J Mol Struct* 1997, 435, 101–107.
20. Kuhn, R.; Ehmann, L. *Helv Chim Acta* 1929, 12, 904.
21. Baranska, M.; Proniewicz, L. M. *J Mol Struct* 1999, 511, 153–162.
22. Schrader, B.; Klump, H. H.; Schenzel, K.; Schulz, H. *J Mol Struct* 1999, 509, 201–212.
23. Schrader, B.; Schulz, H.; Baranska, M.; Andreev, G. N.; Lehner, C.; Sawatzki, J. Online: doi:10.1016/j.saa.2004.10.048.
24. Guineau, B. *Stud Conserv* 1989, 34, 38–44.
25. Tarantilis, P. A.; Beljebbar, A.; Manfait, M.; Polissiou, M. *Spectrochim Acta A* 1998, 54, 651–657.
26. Assimiadis, M. K.; Tarantilis, P. A.; Polissiou, M. G. *Appl Spectrosc* 1998, 52, 519–522.
27. Rodriguez-Amaya, D. B. *Newsletter* 2002, 4, 3–9.
28. Simon, P. W.; Wolff, X. Y. *J Agric Food Chem* 1987, 35, 1017–1022.
29. Ben-Amotz, A.; Fishler, R. *Food Chem* 1998, 62, 515–520.
30. Dumas, Y.; Dadomo, M.; Di Lucca, G.; Grolier, P. *J Sci Food Agric* 2003, 83, 369–382.
31. Milicua, J. C. G.; Juarros, J. L.; De Las Rivas, J.; Ibarrondo, J.; Gomez, R. *Phytochemistry* 1991, 30, 1535–1537.
32. Deli, J.; Molnár, P. *Curr Org Chem* 2002, 6, 1197–1219.
33. Hornero-Méndez, D.; Gómez-Ladrón de Guevara, R.; Mínguez-Mosquera, M. I. *J Agric Food Chem* 2000, 48, 3857–3864.
34. Deli, J.; Molnár, P.; Matus, Z.; Tóth, G. *J Agric Food Chem* 2001, 49, 1517–1523.
35. Buishand, J. G.; Gabelman, W. H. *Euphytica* 1979, 28, 611–632.
36. Burns, J.; Fraser, P. D.; Bramley, P. M. *Phytochemistry* 2003, 62, 939–947.
37. Nechifor, S.; Socaciu, C.; Zsila, F.; Britton, G. *Proceedings of 2<sup>nd</sup> International Congress on Pigments in Food*, Lisbon, 2002; p. 258.
38. Zsila, F.; Deli, J.; Simonyi, M. *Planta* 2001, 213, 937–942.
39. Breithaupt, D. E.; Schwack, W. *Eur Food Technol* 2000, 211, 52–55.
40. Lessin, W. J.; Catigani, G. L.; Schwartz, S. J. *J Agric Food Chem* 1997, 45, 3728–3732.
41. Marx, M.; Stuparic, M.; Schieber, A.; Carle, R. *Food Chem* 2003, 83, 609–617.
42. Baranska, M.; Schulz, H.; Rösch, P.; Strehle, M. A.; Popp, J. *Analyst* 2004, 129, 926–930.
43. Strehle, M. A.; Rösch, P.; Baranska, M.; Schulz, H.; Popp, J. *Biopolymers*, 2004, 77, 44–52.
44. Baranska, M.; Schulz, H.; Siuda, R.; Strehle, M. A.; Rösch, P.; Popp, J.; Joubert, E.; Manley, M., *Biopolymers* 2004, 77, 1–8.
45. Bakó, E.; Deli, J.; Tóth, G. *J Biochem Biophys Methods* 2002, 53, 241–250.
46. Hart, D. J.; Scott, K. J. *Food Chem* 1995, 54, 101–111.
47. Lopez-Hernandez, J.; Vazquez-Oderiz, L.; Vazquez-Blanco, E.; Romero-Rodriuez, A.; Simal-Lozano, J. *J Agric Food Chem* 1993, 41, 1613–1615.

*Reviewing Editor: George J. Thomas*